

New Neutron-Rich Nuclei $^{103,104}\text{Zr}$ and the $A \sim 100$ Region of Deformation

M. A. C. Hotchkis, J. L. Durell, J. B. Fitzgerald, A. S. Mowbray, and W. R. Phillips
Department of Physics, University of Manchester, Manchester M13 9PL, United Kingdom

I. Ahmad, M. P. Carpenter, R. V. F. Janssens, T. L. Khoo, E. F. Moore, and L. R. Morss
Argonne National Laboratory, Argonne, Illinois 60439

Ph. Benet

Purdue University, West Lafayette, Indiana 47907

D. Ye

University of Notre Dame, Notre Dame, Indiana 46556

(Received 5 February 1990)

Partial decay schemes in the neutron-rich nuclei ^{103}Zr and ^{104}Zr have been measured for the first time and rotational bands in $^{100-102}\text{Zr}$ have been extended to spins of up to $10\hbar$ by observing prompt γ rays from the spontaneous fission of ^{248}Cm . These nuclei are among the most deformed known at low spin and excitation energy. The level structures in the odd- A nuclei show that the $h_{11/2}$ intruder orbital plays an important role in stabilizing the deformation in this region.

PACS numbers: 21.10.Re, 23.20.Lv, 25.85.Ca, 27.60.+j

The region of deformation among neutron-rich nuclei with $A \sim 100$ exhibits many interesting features including (1) an abrupt transition from nearly spherical to highly deformed ground states ($\beta_2 \sim 0.4$) in the Zr and Sr isotopic chains¹ at $N=60$; (2) evidence for coexistence of spherical and deformed shapes² near the shape transition; and (3) moments of inertia approaching the rigid-body value, suggesting that the pairing forces are relatively weak in these nuclei. Accounting for these features has proved to be a challenge to theories of nuclear structure. The properties of the Zr isotopes have been discussed^{3,4} in terms of the spherical shell model, the emphasis being on the importance of the isovector neutron-proton interactions between nucleons occupying spin-orbit partner states ($g_{9/2}$ protons and $g_{7/2}$ neutrons) in establishing a stable deformation. These studies suggest that the $h_{11/2}$ intruder orbital is not important at the onset of deformation. On the other hand, calculations using deformed mean fields⁵⁻⁸ indicate that states derived from the neutron $h_{11/2}$ orbital lie well below the Fermi level for large deformations near $N=60$. Hence, the relative importance of the $vh_{11/2}$ and $vg_{7/2}$ states in stabilizing the large ground-state deformations in this region is not clear. Further insight into this problem can be gained in two ways: First, by extending, to higher excitation energy and spin, decay schemes in those neutron-rich nuclei for which only data on low-lying levels are available; second, by examining hitherto unobserved isotopes with large neutron excess in which the occupation probabilities of the important single-particle levels are changed.

At present the neutron-rich nuclei in the $A \sim 100$ region can only be produced for experimental study through fission, and most existing data on them have come from β^- -decay studies of mass-separated fission

fragments. However, recent advances in instrumentation for coincident γ -ray spectroscopy have opened up a new avenue for the study of fission fragments through their prompt radiation. Discrete states in fragments are populated^{9,10} with an average spin of $(6-7)\hbar$, and with sufficiently broad spin distributions that the yrast-level schemes of certain strongly produced fragments can be constructed up to spins of $\sim 12\hbar$. The analysis of prompt γ -ray data from fission has been taken a step further in the present work, with the conclusive assignment of γ -ray transitions to less strongly produced fragments for which there was previously no information, and thereafter the construction of their partial decay schemes. We have for the first time determined partial decay schemes in the nuclei ^{103}Zr and ^{104}Zr , and obtained extensive new data on $^{100-102}\text{Zr}$. The results for ^{102}Zr have also been obtained in a similar experiment, as recently reported.¹¹

Prompt γ rays following the spontaneous fission of ^{248}Cm have been observed using the Argonne-Notre Dame γ -ray facility. This consisted of ten bismuth-germanate-suppressed Ge detectors, two low-energy photon spectrometers (LEPS's), and an array of fifty bismuth-germanate scintillators used as a multiplicity filter. Data were recorded when any two of the Ge or LEPS detectors fired along with at least three elements of the filter. This multiplicity requirement effectively selected prompt fission events, which have an average γ -ray multiplicity of ~ 10 . Almost all events associated with the β decay of fission products are eliminated. The source was a pellet of 11 mm diam containing 5 mg of ^{248}Cm (6.5×10^4 fissions per second), made by mixing curium oxide with 150 mg of potassium chloride and compressing under a pressure of 600 MPa. The curium was chemically purified (separated from fission products)

two days before the experiment started. With the source dimensions given above, the absorption of x rays and low-energy γ rays was limited, while the fragments were stopped quickly so that no Doppler broadening was observed in the γ -ray spectra.

The γ -ray data consist of prompt coincidence events between transitions in a particular nuclear decay sequence and also coincidence events involving transitions in complementary fragments. In spontaneous fission, the primary fragments are produced at a range of excitation energies such that a few neutrons may be evaporated from each fragment. The total number of neutrons emitted per fission event ν typically ranges from 1 to 5. A transition in a given nucleus will therefore appear in coincidence with a number of complementary fragments. Hence, for example, transitions in a range of Zr isotopes will appear in spectra gated on a particular transition in a Ba fragment. While this complicates the coincidence spectra, it also provides a means for identifying the origin of any unknown transition. By studying spectra in

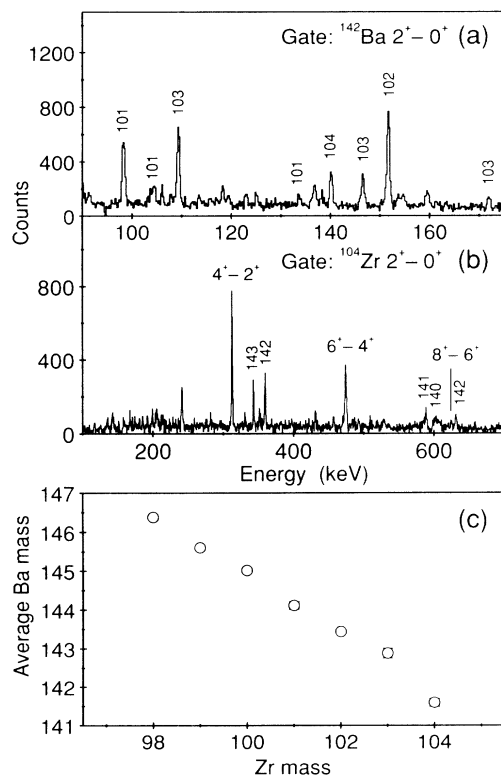


FIG. 1. Examples of data obtained from the fission of ^{248}Cm . (a) Part of a LEPS spectrum in coincidence with the $^{142}\text{Ba } 2^+ - 0^+$ (360 keV) transition; peaks are numbered with the masses of the corresponding complementary Zr fragments. (b) Ge detector spectrum in coincidence with the LEPS peak at 140 keV, which is identified as the $^{104}\text{Zr } 2^+ - 0^+$ transition in ^{104}Zr ; peaks are labeled with the complementary Ba fragment mass or the ^{104}Zr ground-state band transition. (c) Average mass of complementary Ba fragments observed in coincidence with each of the Zr isotopes.

coincidence with transitions in a series of Ba fragments, a sequence of γ rays in different Zr isotopes is observed, among which candidates can be found for transitions in Zr isotopes heavier than those previously known. The procedure is illustrated with an example in Fig. 1. Figure 1(a) is a γ -ray spectrum in coincidence with the $^{142}\text{Ba } 2^+ - 0^+$ transition in ^{142}Ba . This nucleus is lighter than the peak yield for Ba fragments (which occurs at mass 144), and therefore we expect to see the higher-mass Zr isotopes in coincidence. Candidate transitions for $^{103,104}\text{Zr}$ (corresponding to $\nu=3,2$) are indicated along with known γ rays in $^{101,102}\text{Zr}$ ($\nu=5,4$). These candidates are established as belonging to Zr nuclei because spectra obtained in coincidence with them show known transitions in a corresponding range of Ba isotopes, as well as other transitions that can be assembled into a consistent level scheme for that particular Zr isotope. Figure 1(b) shows a spectrum observed in coincidence with the candidate $^{104}\text{Zr } 2^+ - 0^+$ transition. From the relative yields of the Ba fragments seen in this spectrum, the mean value of the Ba mass associated with this transition can be deduced. The same procedure was followed for other transitions proposed in ^{104}Zr as well as for transitions proposed in ^{103}Zr and for known transitions in the lighter Zr isotopes. In Fig. 1(c) the resulting average Ba masses are plotted as a function of the known and proposed Zr masses. A smooth trend is seen, confirming our mass assignments for the new level sequences. Supporting evidence is provided also by the relative yields of the Zr isotopes which approximate a Gaussian distribution with a maximum at ^{101}Zr .

The level schemes of the even-Zr isotopes obtained in this measurement are presented in Fig. 2. These nuclei are among the most deformed known at low spin and excitation energy, with $\beta_2 \sim 0.42$, as derived from the measured¹² lifetime of the 2^+ state in ^{102}Zr . $E(2^+)$ for

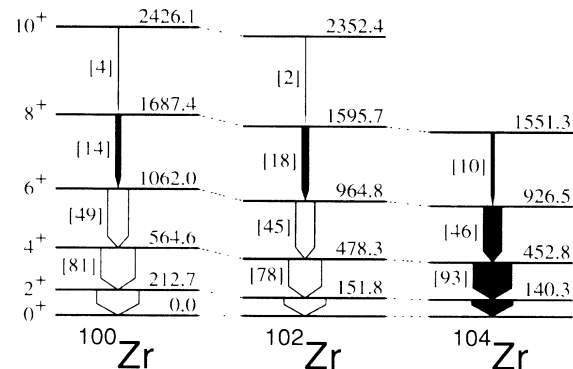


FIG. 2. Level schemes of $^{100,102,104}\text{Zr}$. New transitions observed in this work are shown shaded. γ -ray intensities are given in square brackets relative to 100 γ decays of the first excited state; uncertainties in these vary from $\pm 10\%$ for transitions near the bottom of the bands to $\pm 25\%$ for transitions between the highest spin states observed.

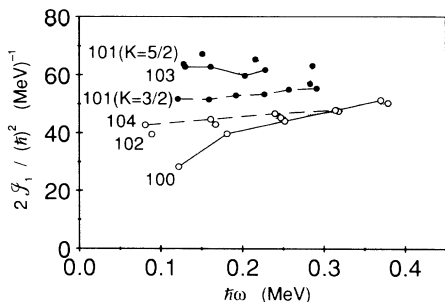


FIG. 3. The kinematic moments of inertia [$2\mathcal{J}_1/\hbar^2 = (4I - 2)/E_\gamma$] plotted as a function of rotational frequency for the observed rotational bands of $^{100-104}\text{Zr}$.

^{104}Zr is lower than that of ^{102}Zr , suggesting that the deformation is larger at the higher neutron excess. ^{104}Zr has an $E(4_1^+)/E(2_1^+)$ ratio of 3.23, the same as that observed¹³ in ^{100}Sr . This value of the ratio is the highest found in this region of nuclei, and close to the theoretical limit of 3.33 expected for a perfect rotor. The data given above have been used to calculate kinematic moments of inertia \mathcal{J}_1 which are plotted as a function of angular frequency in Fig. 3. For all even-Zr isotopes under discussion, the moments of inertia are large and become roughly equal to 60% of the rigid-body value as the rotational frequency increases. The differences in the values of \mathcal{J}_1 at low frequencies are thought to reflect admixture of coexisting spherical configurations into the low-spin states of $^{100-104}\text{Zr}$, and the mixing decreases at higher frequencies. However, some of the deviations could also arise from changes in the pairing field with mass number and/or rotational frequency.¹¹

Well-developed rotational bands are also observed in ^{101}Zr and ^{103}Zr (see Fig. 4). The present work extends substantially the information on the low-lying states in ^{101}Zr reported previously,¹⁴ and transitions in ^{103}Zr have been seen for the first time. The most probable spin-parity values of the levels are indicated, based on the following arguments. In previous work,¹⁴⁻¹⁶ the ground-state bands of the isotones ^{99}Sr , ^{103}Mo , and ^{101}Zr have been assigned to the $\frac{3}{2}^+[411]$ configuration on the basis of feeding patterns in β^- decay and intraband branching ratios. Furthermore, a recent measurement¹⁷ of the ground-state spin and moments of ^{99}Sr confirms the assignment in this case. We note that the excitation energies in the extended band structure of ^{101}Zr reported here strongly support a $K = \frac{3}{2}$ assignment when the level spacings are compared with calculated rotational spacings expected for different K values. Accepting these arguments, the ground-state band of ^{101}Zr is adopted with $K = \frac{3}{2}$ and positive parity. The possible spin values for the 217-keV level of the sideband (Fig. 4) are then limited to $\frac{1}{2}$, $\frac{3}{2}$, $\frac{5}{2}$, and $\frac{7}{2}$. Spin $\frac{1}{2}$ is ruled out because the population intensities of the higher-lying levels in the sideband indicate that this band becomes yrast and spin $\frac{7}{2}$ is excluded on the basis of comparisons with rotational spacings for different K values. With spin $\frac{3}{2}$ for the bandhead, the 321-keV level is expected on the basis of intensity rules for decays to rotational states to decay between 4 and 7 times more strongly to the ground state than to the 98-keV level. In fact, our data put an upper limit of 2% on the ratio of 321- to 223-keV γ rays. A spin of $\frac{5}{2}$ for the 217-keV level leads to no such conflict and is therefore adopted. The sideband most probably has opposite parity to that of the ground-state band, oth-

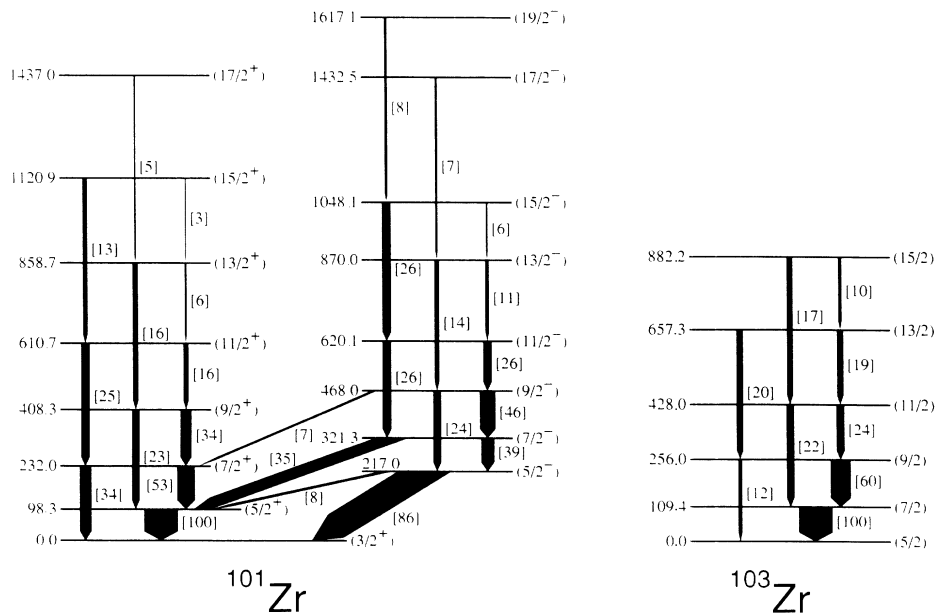


FIG. 4. Level schemes of ^{101}Zr and ^{103}Zr . States with spin $\leq \frac{9}{2}$ in ^{101}Zr were observed in Ref. 14.

erwise Coriolis mixing would be expected which would enhance an $E2$ transition from the 321-keV level to the ground state. Levels of the same spin in the two bands would also be expected to repel each other to a degree; yet pairs of levels with spins $\frac{11}{2}$, $\frac{13}{2}$, and $\frac{17}{2}$ in the two bands are observed very close in energy. Thus, a $\frac{5}{2}^-$ assignment to the head of the sideband is most probable. This band is then associated with the $\frac{5}{2}^-$ [532] intruder configuration ($\nu h_{11/2}$) which is the only one with appropriate spin and parity located near the Fermi surface.⁵⁻⁸ We note that signature splitting is present in the sideband of ^{101}Zr and *not* in the ground-state band. The newly observed band in ^{103}Zr exhibits signature splitting as well, and we propose the same $\frac{5}{2}^-$ [532] configuration. With this assignment, the \mathcal{J}_1 values for these two bands are similar (see Fig. 3).

The configuration assignments given above for the bands in ^{101}Zr and ^{103}Zr are consistent with single-particle energies for neutrons derived from various deformed mean-field calculations,^{5,7,8} and correspond with distinct minima in the predicted potential-energy surfaces^{7,8} at large prolate deformations ($\beta_2 \approx 0.4$). The result that in ^{101}Zr the $\frac{5}{2}^-$ [532] orbital is nearly degenerate with the ground state shows that there is substantial occupancy in ^{100}Zr of the $\Omega = \frac{1}{2}^-$ and $\frac{3}{2}^-$ Nilsson orbitals of the $h_{11/2}$ intruder. In $^{102-104}\text{Zr}$ correspondingly significant occupation of the $\Omega = \frac{1}{2}^-$, $\frac{3}{2}^-$, and $\frac{5}{2}^-$ orbitals is expected. This conclusion supports deformed mean-field calculations which predict that the occupation of the $h_{11/2}$ orbitals near the Fermi surface provides the driving force towards large deformation. It is in contrast with shell-model calculations⁴ which predict that the $h_{11/2}$ orbit has small occupancy and attribute the deformation to the $g_{7/2}$ orbit.

This work was supported by the Science and Engineering Research Council of the United Kingdom under

Grant No. GR.E.6535, by the National Science Foundation under Grant No. PHY88-02279, and by the U.S. Department of Energy under Contracts No. W-31-109-ENG-38 and No. DE-FG02-87ER40346. The authors are also indebted for the use of ^{248}Cm to the Office of Basic Energy Sciences, U.S. Department of Energy, through the transplutonium element production facilities at the Oak Ridge National Laboratory.

¹J. H. Hamilton, in *Treatise on Heavy-Ion Science*, edited by D. A. Bromley (Plenum, New York, 1989), Vol. 8, p. 3; in *Proceedings of the International Workshop on Nuclear Structure of the Zirconium Region*, edited by J. Eberth, R. A. Meyer, and K. Sistemich (Springer-Verlag, Berlin, 1988).

²H. Mach *et al.*, Phys. Lett. B **230**, 21 (1989), and references therein.

³P. Federman and S. Pittel, Phys. Lett. **69B**, 385 (1977); Phys. Rev. C **20**, 820 (1979).

⁴A. Etchegoyen, P. Federman, and E. G. Vergini, Phys. Rev. C **39**, 1130 (1989).

⁵A. Faessler *et al.*, Nucl. Phys. A **230**, 302 (1974).

⁶A. Kumar and M. R. Gunye, Phys. Rev. C **32**, 2116 (1985).

⁷G. Galeriu *et al.*, J. Phys. G **12**, 329 (1986).

⁸P. Bonche *et al.*, Nucl. Phys. A **443**, 39 (1985).

⁹W. R. Phillips *et al.*, Phys. Rev. Lett. **57**, 3257 (1986).

¹⁰Y. Abdelrahman *et al.*, Phys. Lett. B **199**, 504 (1987).

¹¹J. H. Hamilton, in *Microscopic Models in Nuclear Structure Physics*, edited by M. W. Guidry *et al.* (World Scientific, Singapore, 1989), p. 45.

¹²S. Raman *et al.*, At. Data Nucl. Data Tables **36**, 1 (1987).

¹³R. E. Azuma *et al.*, Phys. Lett. **86B**, 5 (1979).

¹⁴F. K. Wohn *et al.*, Phys. Rev. Lett. **51**, 873 (1983).

¹⁵K. Shizuma *et al.*, Z. Phys. A **315**, 65 (1984); T. Seo *et al.*, Z. Phys. A **320**, 393 (1985).

¹⁶B. Pfeiffer *et al.*, Z. Phys. A **317**, 123 (1984); G. Lhersonneau *et al.*, Z. Phys. A **332**, 243 (1989).

¹⁷P. Lievens *et al.* (to be published).